Lung CT Image Segmentation Using VGG-16 Network with Image Enhancement Based on Bounded Turning Mittag-Leffler Function

Ali M. Hasan*[1], *Mohammed Khalaf [2]*, *Bayan M. Sabbar[3]*, *Rabha W. Ibrahim [4,5,6]*, *Hamid A. Jalab[6]*, *Farid Meziane[7]*

[1]Department of Physiology and Medical Physics, College of Medicine, Al-Nahrain University, Baghdad, Iraq.
[2]Department of Computer Science, Al-Maarif University College, Al Anbar, Iraq.
[3]College of Engineering and Engineering Techniques, Al-Mustaqbal University, Babylon, Iraq.
[4]Department of Computer Science and Mathematics, Lebanese American University, Beirut, Lebanon.
[5]Department of Mathematics, Mathematics Research Center, Near East University, Mersin, Turkey.
[6]Information and Communication Technology Research Group, Scientific Research Center, Alayen University, Thi Qar, Iraq.
[7]Data Science Research Centre, School of Computing and Engineering, University of Derby, UK.

Abstract

Automated segmentation of diseases considered a necessary initial step in routine diagnosis. Lung diseases that affect the lungs, such as pneumonia or lung collapse can result in areas of consolidation or atelectasis, where lung tissue becomes denser or collapses. It can be challenging to accurately segment such areas, as they may exhibit similar characteristics to adjacent structures. This study proposes a lung CT image segmentation method which includes two steps: (1) a new image enhancement model that uses the bounded turning Mittag-Leffler function to improve the CT images for better segmentation outcomes. (2) a new modified VGG-16 for infection of lung segmentation based on expanding the original VGG-16 network. The dilated convolutional layers are added to the original VGG-16 network to create a new lung CT image segmentation method. The experimental results showed that the proposed method can accurately segment the infected region in lung CT scans. The results led to Accuracy, Dice Coefficient and Jaccard Index values of 96.3%, 91.2%, and 82.3% respectively. The proposed method is accurate and suitable for implementation in real-world applications. Following result computation, seven related studies are compared with the recommended methodology. This demonstrated how well this study had performed in comparison to many earlier studies. Despite the fact that segmenting lung CT images requires a lot of work. Obtaining a suitable level of accuracy was quite difficult.

Keywords: Bounded turning, CT scans, Image Enhancement, Mittag-Leffler function, VGG-16 network.

Introduction

The CAD (computer-aided diagnosis) systems have been used to aid medical professionals in the diagnosis of a variety of lung diseases [1]. There are four main steps of the CAD system: the preprocessing of input images; identifying the region of interest (ROI); extracting features from the ROI, and then classifying the features using a practical classifier [2]. Due to its capacity to obtain textural details of the lung morphology in diagnosis process, CT imaging is frequently used. However, its accuracy heavily relies upon the quality of the obtained images, as well as the expertise of

radiologists. The clinical applications of CT have expanded dramatically because of increasing image quality and decreasing acquisition times. The most crucial component of medical imaging is an image segmentation. Developing an automated segmentation system that is based on CT scans of the lungs remains a challenging process, as the contrast between the lesion, the surrounding healthy tissue, the ribs, and the large pulmonary blood vessels is extremely low. The accurate segmentation of CT scans of the infected lungs plays an essential role in the prognosis and outcome of the disease. Based on these observations, this study proposes a new image enhancement technique that combines the expanding VGG-16 CNN network with the bounded turning Mittag-Leffler function to segment the infected region in lung CT scans.

Image enhancement involves performing adjustments to digital images to make them more suitable for image analysis. The goal of image enhancement is to improve the brightness, contrast, and sharpness of input image. Image enhancement technique is applied as a pre-processing step before image classification task [3,4]. The fractional calculus operators have been applied as a novel method for improving images by [5, 6]. Regardless of how the fractional operators perform as image enhancing models, an improvement is still conceivable. The study of proposed by Jimin et al [7] applied a new entropy based on pixel probability of nearby pixels. This method produced good outcomes. In new approach, Ibrahim et al, [5] introduced a novel fractional partial differential class for low contrast images of the brain and lungs, CT scan datasets of varying quality as a new image enhancement method. This method, however, requires low-resolution photos to enhance the image. A new fractional Rényi entropy model was proposed by Kumar et al, [8] to enhance the final reconstructed MR image. To address the problems of CT scan image enhancement, in this study, it is proposed a new image enhancement model that uses the bounded turning Mittag-Leffler function proposed as pre-processing stage for better segmentation outcomes.

Image segmentation models are important techniques in the field of image processing and are useful in many applications. Image segmentation essentially can be classified into two main types: traditional, and those based on deep learning. The traditional type can be further classified into two broad categories namely "region-based segmentation" and "edge-based segmentation" techniques. As in many medical imaging there is a move to the use of deep learning models for image segmentation as these have been shown to outperform traditional models [9, 10]. Recent research involving neural networks-based deep-learning techniques have facilitated the emergence of high-performance algorithms for semantic segmentation and instance segmentation. The growing number of researchers have demonstrated that deep learning-based CNN-based medical image segmentation models have a remarkable ability to detect and segment infections from lung CT scans [11]. Fan, et al. [12] presented a semi-automated deep network (Semi-Inf-Net) for the segmentation of "COVID-19" lung infection. The proposed network uses a "parallel partial decoder" to obtain high-level features from the input image, then generates a global map that is used to model the boundaries of the infected area. The maximum achieved segmentation Dice-score of classifying 100 labeled "COVID-19" CT images was 73.9%. Shan, et al. [13], proposed an automated DL-based system for the segmentation and qualification of "COVID-19" infected regions in CT scans of lungs. The system is based on the VB-Net neural network, and it was reported that it achieved a Dice-score of 91.6% when tested with 249 CT images of infected "COVID-19" patients. In a recent study, Saood and Hatem [14], presented a set of deep learning networks: SegNet and U-Net for image tissues segmentation. The former has been employed to segment a scene whereas the latter has been used as a medical segmentation tool. Both deep learning networks were utilized as binary segmenters to recognize the infected lung tissue by "COVID-19". The achieved accuracies were 95% and 91% by SegNet and U-Net respectively when tested with a dataset comprising one-hundred CT slices of infected lung by "COVID-19". Similarly, Budak, et al. [15], utilized the attention gate (AG) mechanism to propose a SegNet-based network for the automated segmentation of infected "COVID-19" regions in CT scans of lung. The obtained dice score of segmenting a dataset that included 473 labeled CT images was 89.61%. In a similar work, Raj, et al. [16], proposed the "attention Gate-Dense network- improved dilation convolution- U-Net" (ADID-UNET) for "COVID-19" infection segmentation. The experimental results showed that the system managed to achieve a dice score of 80.31% when tested with a dataset that is composed of 100 axial

CT scans belonging to a different set of "COVID-19" patients.

A 3D U-Net model for tumor segmentation in CT images was presented in Le and Saut [17] study. A small set of CT scans was used to train the study from beginning to end, and a different set of CT scans was used for validation. The outcomes of the experiment demonstrated that this model is capable of providing a very precise tumor segmentation in the three-dimensional volume of CT images. However, the main limitation and challenges associated with the use of U-Net 3D for lung tumor segmentation is the computational Load which required significant memory. Similarly, a novel lung segmentation algorithm based on a dilated U-Net approach was presented in the study by Liu and Pang [18]. To create precise lung contours, the lung regions were first extracted using a double-dilated U-Net model. After that, a novel multi-scale gray correlation-based segmentation method was used to obtain the first nodule contours. Lastly, a level set method was used to refine the contours of the lung nodules. According to experimental results, when compared to ground truth, the suggested algorithm generates an average Dice similarity coefficient of 72.14%. Dilated convolutions have the potential to improve multi-scale information capture when added to the U-Net model. Finding the ideal dilation rate, an extra hyperparameter to adjust that may vary depending on

the application, is the primary drawback and difficulty of using U-Net 3D for lung tumor segmentation.

To address the problems of lung segmentation, a fully automated and efficient transfer learning based deep CNNs is proposed, which is trained on a large dataset of natural images (ImageNet). VGG-16 is known as "Very Deep Convolutional Networks for Large-Scale Image Recognition". Its ImageNet dataset contains more than 14 million images for 1000 classes. The dilated convolutional layers, which increase the receptive fields of CNNs by inserting zeros, have been added to the transfer learning-based deepVGG-16 network to improve segmentation accuracy. The contributions are as follows:

1. To overcome the problem of blurry edges, a new image enhancement model using bounded turning Mittag-Leffler function is proposed to enhance the CT images for better segmentation of infected areas.

2. To address the problem of extracting an efficient segmentation, the pre-trained VGG-16 is applied instead of a traditional CNNs in which the low training parameters of the VGG-16 network reduced the time complexity cost.

Materials and Methods

The pre-processing of CT images and the VGG-16 to segment the infected lung region are the two main stages of the proposed study.

1. CT Lung scan pre-processing

Medical images, such as CT scans, often suffer from various types of noise, artifacts, and inconsistencies. The artifacts can influence the quality of the scan and may lead to variations in intensity that occur between successive slices of CT scans. These issues can make it challenging to accurately identify and differentiate different structures and regions within the image. Lung CT scans are widely used in the diagnosis, staging, and treatment of a wide range of pulmonary conditions. These scans can be pre-processed to improve the information content and image quality, which can significantly improve the analysis that follows whether it is done automatically by computer algorithms or manually by radiologists. One of the main functions of pre-processing is segmentation,

which involves separating or segmenting various structures such as the bronchi, lung parenchyma, nodules, and chest wall. Accurate segmentation can improve the accuracy of subsequent analysis. Therefore, image enhancement techniques are employed to improve the quality and enhance the relevant features in medical images. In order to decrease the likelihood of pixels being incorrectly classified by VGG-16 and improve segmentation performance, it is crucial to reduce the effects of these causes prior to any segmentation process. All CT lung slices are enhanced by proposed bounded turning Mittag-Leffler function as new enhancement method to reduce intra-scan and inter-scan image variations [19]. In many different facets of image processing, complex differential equations (CDEs) are crucial. For processes like image enhancement, they are especially helpful.

One of the important concepts in CDEs is the bounded turning functions (BTFs). A function that

maps complex numbers to complex numbers and demonstrates the property of BT is known as a BTF of a complex variable. The most popular example of such a function is e^{i*z}. Although the argument of z is multiplied by i, the modulus of z is preserved. The complex plane is rotated by the argument of z as represented by the exponential function e^{i*z}. The resultant argument, nonetheless, will be raised by a predetermined number of 90 degrees (or /2 radians) in the counterclockwise direction because the argument of z is multiplied by i. The BTFs are mathematical functions utilized in image processing to find edges and boundaries in an image. This study uses the generalized BTF called the Mittag-Leffler function.

$$E_a(i*z) = 1 + \frac{iz}{\Gamma[1+a]} - \frac{z^2}{\Gamma[1+2a]} + z^3\left(-\frac{i}{\Gamma[1+3a]} + z\left(\frac{1}{\Gamma[1+4a]} + \frac{iz}{\Gamma[1+5a]} - \frac{z^2}{\Gamma[1+6a]}\right)\right) \qquad 1$$

Remark 1

The bounded turning Mittag-Leffler function is a fractional calculus and fractional differential equation's special function. It is a variant of the more familiar Mittag-Leffler function. The overall set of fractional differential equations may be described using the bounded turning Mittag-Leffler function. In the same manner that the regular Mittag-Leffler function is utilized to solve ordinary fractional differential equations, the bounded turning Mittag-Leffler function is helpful for solving such fractional differential equations. As a result, the bounded turning Mittag-Leffler function is a sophisticated mathematical function utilized during fractional calculus that has significance for sciences, engineering, and statistical analysis. When compared to standard functions, it is an extra generic and versatile tool for computing fractional differential equations.

Proposition 1

The terms of the BTF $E_a(i*z), a > 0$ (the fractional power) can be bounded in the open unit disk ($|z|=r<1$, where r indicates the probability of the pixel), as follows:

$$t_0 = 1; \ |t_1| \leq \frac{r}{\Gamma[1+a]} \ ; |t_2| \leq \frac{r}{\Gamma[1+2a]} ; \dots ; |t_n| \leq \frac{r}{\Gamma[1+na]}$$

Proof.

Clearly, by using the series in (1), t_0 will be equal **1**. For the second term

$$t_1 = \frac{iz}{\Gamma[1+a]} \ \rightarrow \ |t_1| \leq \frac{|iz|}{\Gamma[1+a]} \ \leq \frac{r}{\Gamma[1+a]}.$$

Similarly, for t_2

$$t_2 = \frac{-z^2}{\Gamma[1+2a]} \ \rightarrow \ |t_2| \leq \frac{|-z^2|}{\Gamma[1+2a]} = \frac{|z|^2}{\Gamma[1+2a]}$$
$$= \frac{r^2}{\Gamma[1+2a]} \leq \frac{r}{\Gamma[1+2a]}.$$

In general, Eq.2 and Eq. 3 are achieved.

$$|t_n| \leq \frac{r^n}{\Gamma[1+na]} \leq \frac{r}{\Gamma[1+na]}, \ r < 1 \qquad 2$$

$$T_{n,m}(i,j) = \sum_{i=1}^{n}\sum_{j=1}^{m} G(i,j) \times \frac{r}{\Gamma[1+na]} \qquad 3$$

Where $G(i,j)$ is the input image, a>0 is the fractional power, and r indicates the probability of the pixel. The fractional power (a) empirically determined value of 0.75 was selected to produce the best enhanced results. The goal of proposed image enhancement is to improve the visual quality and clarity of images. The proposed enhancing method's qualitative results are shown in Fig. 1. After the improvement process, areas that lack details become brighter and more distinct. The properties of the original and enhanced images differ, as shown by the histogram analysis.

2. The proposed transfer learning-based segmentation

The transfer learning is used in this study to exploit the acquired knowledge of VGG-16 to solve different related problems by using different sets of data. The VGG-16 network includes a stack of 13 convolutional (conv) layers organized as follows:

- The first two convolutional layers (conv 1-1 and conv 1-2) are of size (224×224) with 64 kernel filters.
- The second two convolutional layers (conv 2-1 and conv 2-2) are of size (112×112) with 128 kernel filters.
- The third three convolutional layers (conv 3-1, conv 3-2 and conv 3-3) are of size (56×56) and 256 kernel filters.

- The fourth three convolutional layers (conv 4-1, conv 4-2 and conv 4-3) are of size (28×28) and 512 kernel filters.
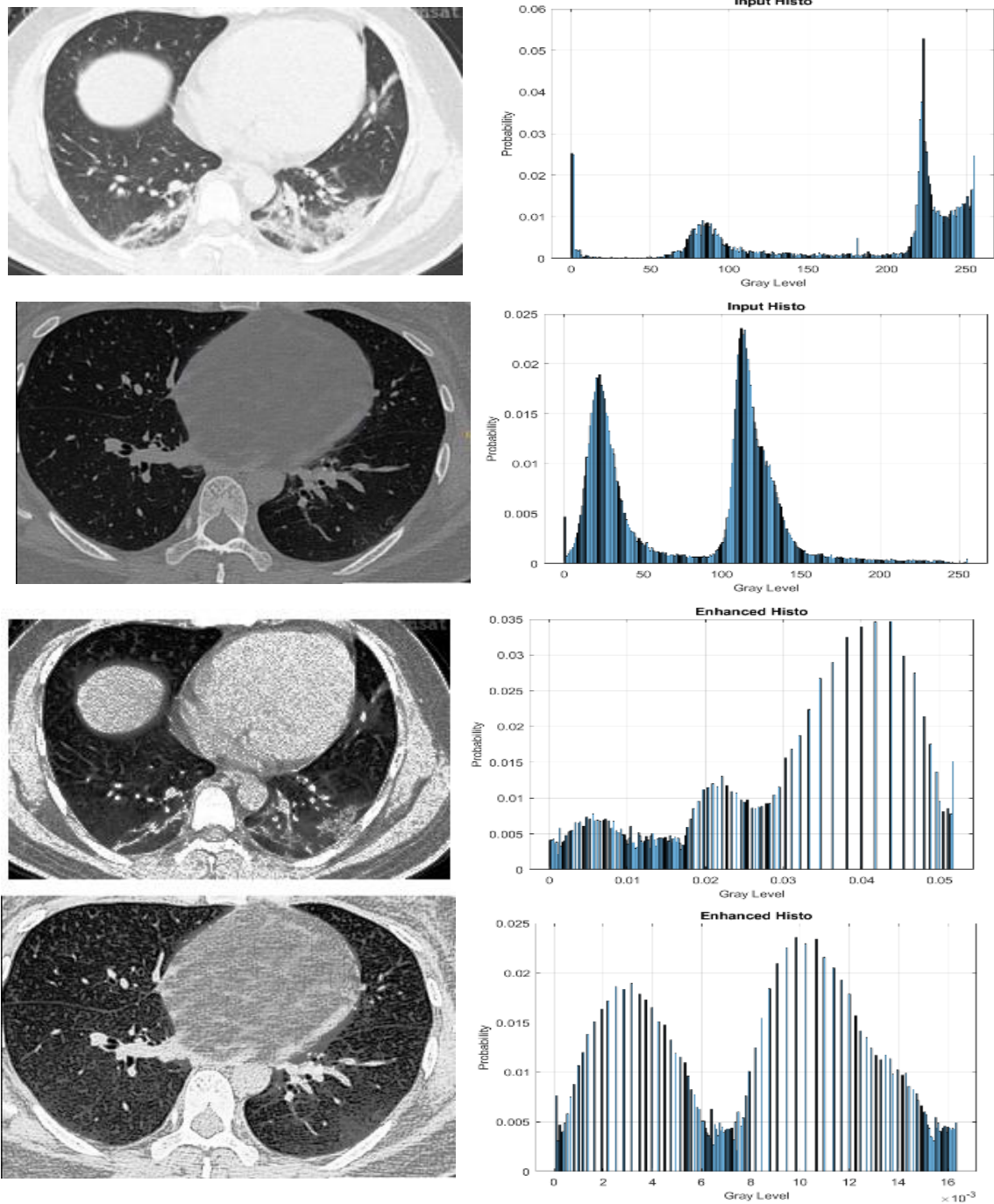

Figure 1. The histogram outcomes, input, and enhanced images.

- The fifth three convolutional layers (conv 5-1, conv 5-2 and conv 5-3) are of size (14×14) and 512 kernel filters.
- The fourth three convolutional layers (conv 4-1, conv 4-2 and conv 4-3) are of size (28×28) and 512 kernel filters.

- The fifth three convolutional layers (conv 5-1, conv 5-2 and conv 5-3) are of size (14×14) and 512 kernel filters.

For all kernel filters of size (3×3), the convolution stride is fixed to one pixel, and the number of zero-padding is fixed in a way that the spatial resolution is

preserved after each convolution. Finally, three fully connected (FC) layers follow multi convolutional layers that have a different depth in different architectures. The final layer is the SoftMax layer. The configuration of the full layers of the VGG-16 network is shown in Fig. 2-A.

The proposed network is a customized version of the VGG-16 network. Since the original VGG-16 was trained for the image classification task, it must be modified for the segmentation task. The use of the max-pooling layers periodically within the VGG-16 network leads to reducing the spatial size periodically by a factor of 32 until reaching the fully connected layers as shown in Fig. 2-B.

The last three fully connected layers were replaced by three convolutional layers Conv 6-1, Conv 6-2, and Conv 6-3 of size (7×7) and 512 kernel filters. Where, the feature maps of the latter include a coarse prediction or confidence maps. A fine prediction can be obtained by combining the Conv 6-3 layer with that of shallower layers. So, (1×1) convolutional layers (termed here as Conv 7 and Conv 8) were used respectively for dimensionality reduction to remove computational bottlenecks from the pooling layers' outputs (Pooling 3 and Pooling 4), in order to be summed with the outputs of the two convolutional transpose layers (termed here as Conv Trans 7 and Conv Trans 8 of size (56×56) and 256 kernel filter) with up sampling factor of (2×2) respectively and produce predictions at higher resolutions of (28×28×512) and (56×56×256) respectively. Then, another convolutional transpose layer (Conv Trans 9) with an up-sampling factor of (4×4) was used to produce a final prediction at the same spatial size of lung CT images (224×224×64). With a SoftMax layer that generates per-pixel class probability estimates infection in lung CT image label, the proposed network was completed.

3. Evaluation metrics

The accuracy (ACC), Dice Coefficient (DC), and Jaccard Coefficient (JC) are used as metrics to evaluate the segmentation performance of the proposed network. The three main metrics used to assess the quality of image segmentations are accuracy, jaccard, and dice coefficients. They are extensively employed in both theoretical and practical contexts, providing information about the degree of overlap between predicted and ground truth segmentations, assisting researchers in optimizing segmentation algorithms, and assisting decision-makers in domains like medical imaging. These metrics represent the degree of similarity between the lung areas segmented using the algorithm to the ground truth based on the True Positive (TP), False Positive (FP), True Negative (TN), and False Negative (FN). Here, TP represents the number of pixels that are correctly segmented as part of an infected area, FP represents the total count of pixels that are inaccurately segmented as part of infected area. Similarly, TN represents the total number of pixels that are correctly segmented as part of the healthy area.

$$ACC = \frac{TP+TN}{TP+TN+FP+FN} \qquad 4$$

$$DC = \frac{2|Seg \cap Ref|}{|Seg \cup Ref|} = \frac{2TP}{2TP+FP+FN} \qquad 5$$

$$JC = \frac{|Seg \cap Ref|}{|Seg ? Ref|} = \frac{TP}{TP+FP+FN} \qquad 6$$

4. Image Dataset

The image datasets used in this study are publicly available dataset used for image processing and machine learning research. In the field of medical image classification, researchers often used these datasets to train and test algorithms that can segment and detect lung diseases in CT scans. These datasets provide many types of lung diseases in CT scans, making it valuable resource for developing and benchmarking lung diseases segmentation and detection algorithms. All the provided CT scans were segmented by the "Italian society of medical and interventional radiology's radiologists" [20]. Another dataset from [21] was used in this study. It includes segmented labels of 373 out of 829 axial CT slices. The whole dataset that was used in this study was divided randomly into 70% for training and 30% for testing. To train the proposed network, all lung CT images, and their ground truth labels were resized to (72×72) pixels.
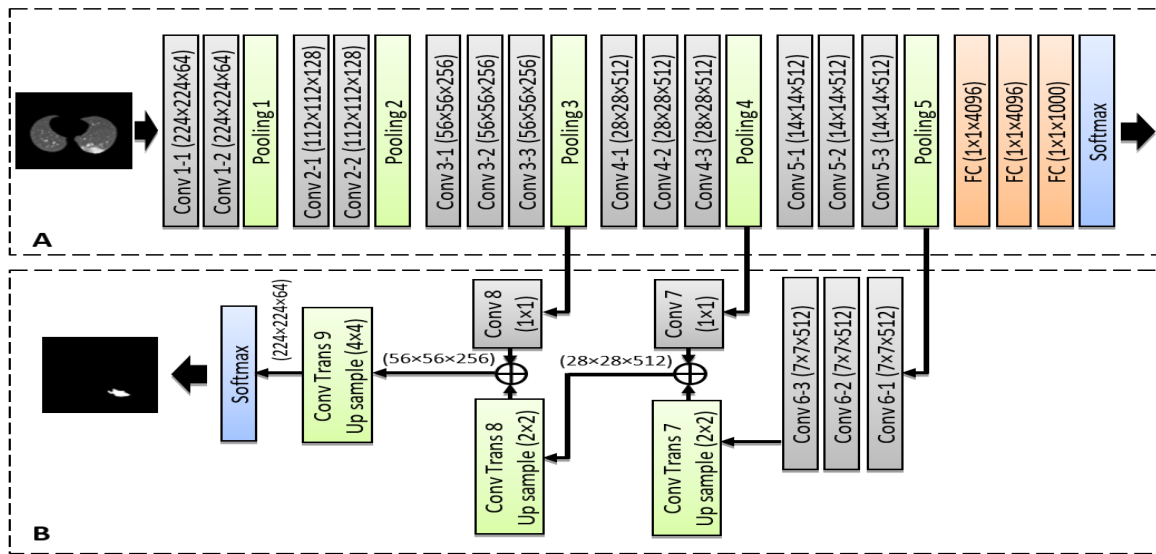
Figure 2. The Proposed segmentation model: (A) the original structure of VGG-16 network (B) the infection in lung CT scans segmentation branch.

Results and Discussion

The CT scans in the dataset have been used for both training (70%) and testing (30%) stages. Five-fold cross-validation is implemented in which the CT scan dataset is divided into five subsets. The codes were developed in Matlab 2021a running on an Intel i7-6700HQ (2.6 GHz) 64-bit Windows 10 machine with 16GB RAM and NVIDIA GTX 950 GPU.

Reducing the training image size by bilinear interpolation will help in reducing the processing time of the proposed network. By utilizing a set of augmentation techniques like resizing, rotation, and reflection, various variations of each original training CT image were generated in order to reduce overfitting and improve the network's generalization. The range of rotations was picked up randomly for each image by rotating the image within a specified interval between -180º to 180º without resizing.

Part A Fig. 2-A of the proposed network was initialized with the original weights from VGG-16, that has been trained on millions of images. The weights of part B Fig. 2-B were randomly initialized using the Xavier algorithm with biases set to zero initially. The Xavier algorithm is used to initialize the weights of the network with smarter values that prevent neurons to be trapped in saturation during training. Generally, the standard stochastic gradient-descent (SGD) based optimization algorithm is used to drop the errors of the proposed network and produces an extremely improved weight. After successfully training, the test CT images with the result of the manual segmentation as the gold

standard, these were fed into the proposed trained network for segmentation evaluation. Fig 3, shows how the proposed network was trained successfully on the provided CT images of patients with lung diseases as shown in Fig. 4, where the predicted output of the proposed network is compared with the corresponding ground truth image to determine the total number of the correctly segmented pixels.

The ground truth provided with the downloaded dataset are marked in red, and the boundaries of the infected area and recognized by the proposed network are marked in yellow. As mentioned above, three measures ACC, DC and JC are used to evaluate the segmentation for all the 143 CT images then averaged to obtain average coefficients scores as shown in Table 1.
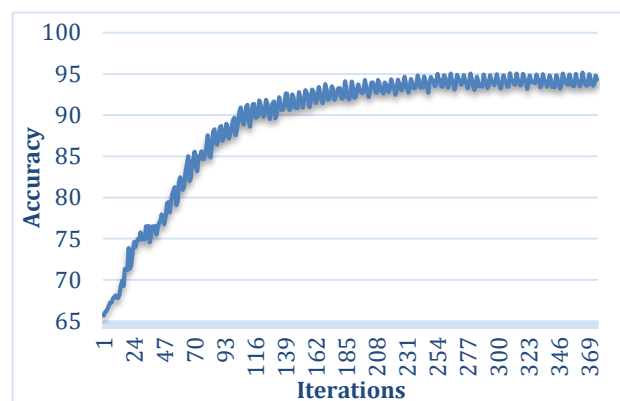

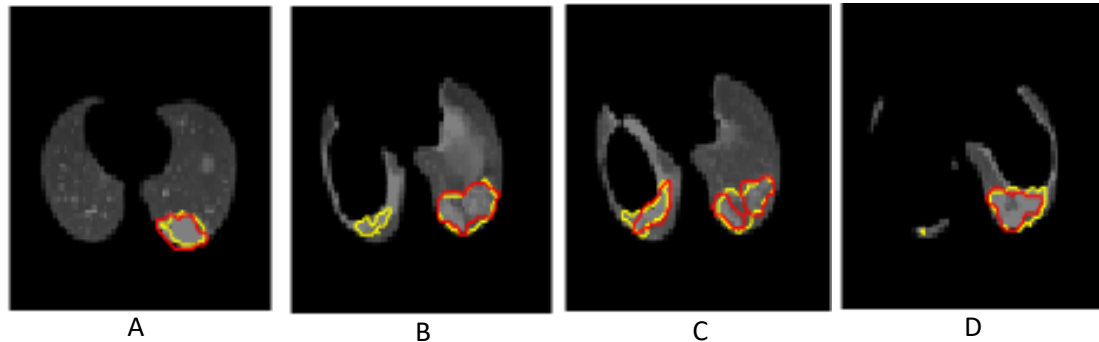**Figure 3. The training process of the proposed network.**

Figure 4. Comparative segmentation results, the ground truth image is in red, and the segmented is in yellow, A) Segmented with 95% accuracy, B) Segmented with 90% accuracy, C) Segmented with 91% accuracy, and D) Segmented with 96% accuracy.

Table1. Segmentation results of "COVID-19"143 CT images from the downloaded dataset.

Results	Accuracy	Dice Index	Jaccard
Average	0.963	0.912	0.823
STD	0.082	0.052	0.075
Min	0.906	0.746	0.643
Max	0.993	0.955	0.944

The proposed network was successfully applied to the downloaded dataset. The ACC, DC, and JC were 96.3%±8.2%, 91.2%±5.2%, and 82.3%±7.5% respectively. The achieved results of Dice coefficient illustrated the precision of image segmentation in which the predicted segmentation and the ground truth segmentation are compared to see how similar or overlapped they are.

Stages of lung disease and the effects of increasing slice thickness of scanning were the primary challenges encountered during segmentation, as shown in Fig. 5. Where, the scatter plot shows a negative correlation between the achieved accuracy and the slice thickness. Therefore, to achieve a high segmentation accuracy, a reduction of the slice thickness is essential. Furthermore, the infected regions do not have clear boundaries at early stages and could present with a higher variance in the volume when compared to infected regions from later stages of the disease. To evaluate the effectiveness of segmenting lung infection CT scans, the results of the proposed segmentation method are compared with various lung segmentation techniques, as shown in Table 2.
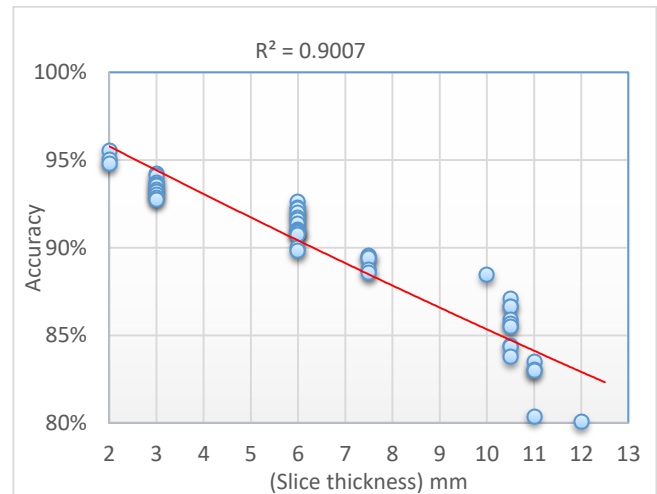

Figure 5. Scatter plot of accuracy to the slice thickness of the slices, showing mean of accuracy (R2) as the dotted red line.

Table 2. Results of proposed lung CT scans segmentation and other lung segmentation techniques.

Ref.	Approach	Accuracy (%)	Dice (%)
12	Semi-Inf-Net	-	73.9
22	LungINFseg network	-	80.34
14	SegNet	95	-
	U-Net	91	-
15	SegNet	-	89.61
16	ADID-UNET	-	80.31
13	VB-Net neural network	-	91.60
Proposed	Modified Transfer Learning (VGG-16)	96.3	91.2

As it can be seen, the dice metrics output of the proposed segmentation model outperforms the Fan, et al. [12] who provided a semi-automated deep network (Semi-Inf-Net) for the segmentation of lung infection of a dataset that included 100 CT images. To segment the infections in lung CT images [22],

introduced LungINFseg, a fully automated and effective deep learning-based method. Over the entire collected dataset which included 19 CT images, the achieved dice score was 80.34%. Whereas, SegNet and U-Net networks were used by Saood and Hatem [14], as a binary segmentor network to discriminate between infected and healthy lung tissue, and the achieved accuracies of segmenting 100 CT by both networks were 95% and 91% respectively. Budak, et al. [15] and Raj, et al. [16] utilized the attention gate (AG) mechanism to propose SegNet-based networks for the automated segmentation of infected regions in CT scans of lung. Where, Budak and Raj achieved Dice scores of 89.61% (473 CT images of lung) and 80.31% (100 CT images of lung) respectively. However, the dice metrics achieved by Shan et al. [13] which used the VB Net neural network with 249 CT images was better than the proposed method. This is possibly due to the small number CT images used by Shan, et al. [13] compared to our dataset. Comparing with Saood and Hatem [14] the proposed lung CT scan segmentation model has the better segmentation accuracy, which indicated its excellent performance. The experimental results showed that the suggested lung CT scan segmentation model performs better in segmentation and significantly improves in accuracy and dice metrics.

Conclusion

A crucial stage in many computer-aided diagnostic systems for lung diseases is lung segmentation in CT scans. Accurate segmentation aids in distinguishing the lungs from surrounding tissues, improving the precision of later analyses. In this study, a new modified VGG-16 for infection of lung segmentation based on expanding the original VGG-16 network with a new image enhancement model based on bounded turning Mittag-Leffler function to eliminate the irrelevant pixels in an axial view of a CT scan was proposed. Combining VGG-16 and dilated convolution has led to an enlarged receptive fields of segmentation model by inserting zeros in the CNN filters, which has no computational cost. The accuracy, Dice coefficient, and Jaccard index values attained through the suggested CNN structure were 96.3%, 91.2%, and 82.3%, respectively. Results demonstrate that the proposed network outperforms the existing lung infection segmentation methods. Accurate lung segmentation holds great potential for the future, going beyond simple diagnostics. It can be used for sophisticated applications like radiation therapy planning, surgical planning, and long-term studies to monitor the effectiveness of treatments or the progression of disease. For future improvements include using other medical imaging formats (e.g., X-ray and MRI scans) while maintaining the same level of segmentation efficiency, as well as using larger datasets of public multiple lung diseases in CT images with ground truth.

Acknowledgments

Authors' Declaration

- Conflicts of Interest: None.
- We hereby confirm that all the Figures and Tables in the manuscript are ours. Furthermore, any Figures and images, that are not ours, have been included with the necessary permission for re-publication, which is attached to the manuscript.
- Ethical Clearance: The project was approved by the local ethical committee at Al-Nahrain University.
- Ethics statement:
- No animal studies are present in the manuscript.
- No human studies are present in the manuscript.
- No potentially identified images or data are present in the manuscript.

Authors' Contribution Statement

References

1. Salama GM., Mohamed A., Abd-Ellah MK. COVID-19 classification based on a deep learning and machine learning fusion technique using chest CT images. Neural Comput & Applic. 2024; 36, 5347–5365. https://doi.org/10.1007/s00521-023-09346-7.

2. Aggarwal P., Mishra NK., Fatimah B., Singh P., Gupta A., Joshi SD. COVID-19 image classification using deep learning: Advances, challenges and opportunities. Comput Biol Med. 2022; 144, 105350. https://doi.org/10.1016/j.compbiomed.2022.105350.

3. Hasan AM, Qasim AF, Jalab HA, Ibrahim RW. Breast Cancer MRI Classification Based on Fractional Entropy Image Enhancement and Deep Feature Extraction. Baghdad Sci J. 2022; 0221-0221. https://doi.org/10.21123/bsj.2022.6782.

4. Fadhil OY, Mahdi BS, Abbas AR. Using VGG Models with Intermediate Layer Feature Maps for Static Hand Gesture Recognition. Baghdad Sci J. 2023. https://doi.org/10.21123/bsj.2023.7364

5. Ibrahim RW, Jalab HA, Karim FK, Alabdulkreem E, Ayub MN. A medical image enhancement based on generalized class of fractional partial differential equations. Quant Imaging Med Surg. 2022; 12 (1): 172 . https://dx.doi.org/10.21037/qims-21-15

6. Cao J. An Image Enhancement Method Based on Fractional Calculus and Retinex. JCC. 2018; 6 (11), pp.55-65. http://doi.org/10.4236/jcc.2018.611005.

7. Yu J., Tan L., Zhou S., Wang L., Siddique MA. Image denoising algorithm based on entropy and adaptive fractional order calculus operator. IEEE access. 2017; 5: 12275-12285. https://doi.org/10.1109/ACCESS.2017.2718558.

8. Kumar PA., Gunasundari R., Aarthi R. RE-SHFC: Renyi Entropy-Based Spotted Hyena Fractional Calculus Algorithm for MR Image Reconstruction. Sensing and Imaging. 2022; 23(1): pp. 8. https://doi.org/10.1007/s11220-022-00377-3

9. Gupta M., Mishra A. A systematic review of deep learning based image segmentation to detect polyp. Artif Intell Rev. 2024; 57 (7). https://doi.org/10.1007/s10462-023-10621-1

10. Alnedawe SM, Aljobouri HK. A New Model Design for Combating COVID-19 Pandemic Based on SVM and CNN Approaches. Baghdad Sci J. 2023; 20 (4): 1402-1413. https://doi.org/10.21123/bsj.2023.7403

11. Gite S., Mishra A., Kotecha K. Enhanced lung image segmentation using deep learning. Neural Comput & Applic. 2023; 35, 22839–22853. https://doi.org/10.1007/s00521-021-06719-8

12. Fan D-P, Zhou T, Ji G-P, Zhou Y, Chen G, Fu H, et al. Inf-net: Automatic covid-19 lung infection segmentation from ct images. IEEE Trans Med Imaging. 2020; 39 (8): 2626-2637. https://doi.org/10.1109/TMI.2020.2996645

13. Shan F, Gao Y, Wang J, Shi W, Shi N, Han M, et al. Lung infection quantification of COVID-19 in CT images with deep learning. arXiv preprint arXiv:2003.2020; 04655 . https://doi.org/10.48550/arXiv.2003.04655

14. Saood A, Hatem I. COVID-19 lung CT image segmentation using deep learning methods: U-Net versus SegNet. BMC Med Imaging 2021; 21 (1): 1-10. https://doi.org/10.1186/s12880-020-00529-5

15. Budak Ü, Çıbuk M, Cömert Z, Şengür A. Efficient COVID-19 segmentation from CT slices exploiting semantic segmentation with integrated attention mechanism. J Digit Imaging .2021; 34: 263-272. https://doi.org/10.1007/s10278-021-00434-5

16. Raj ANJ, Zhu H, Khan A, Zhuang Z, Yang Z, Mahesh VG, et al. ADID-UNET—a segmentation model for COVID-19 infection from lung CT scans. PeerJ Comput Sci.2021; 7: e349. https://doi.org/10.7717/peerj-cs.349

17. Le V-L, Saut O, editors. RRc-UNet 3D for Lung Tumor Segmentation from CT Scans of Non-Small Cell Lung Cancer Patients. ICCV CVAMD 2023 - Workshop of International Conference on Computer Vision, Oct 2023, Paris, France.2023; pp.2316-2325. https://doi.org/10.1109/ICCVW60793.2023.00245

18. Liu C, Pang M. Lung CT Image Segmentation via Dilated U-Net Model and Multi-scale Gray Correlation-Based Approach. Circuits Syst Signal Process.2023; 1-18. https://doi.org/10.1007/s00034-023-02532-x

19. Petráš I. Novel Low-Pass Two-Dimensional Mittag–Leffler Filter and Its Application in Image Processing. Fractal and Fractional. 2023; 7(12): pp. 881. https://doi.org/10.3390/fractalfract7120881

20. COVID-19, Medical Segmentation. 2021. https://www.kaggle.com/competitions/covid-segmentation/data.

21. Sharif PM, Nematizadeh M, Saghazadeh M, Saghazadeh A, Rezaei N. Computed tomography scan in COVID-19: a systematic review and meta-analysis. Pol. J. Radiol.Feb 2022;87:e1–23. https://doi.org/10.5114%2Fpjr.2022.112613

22. Singh V, Abdel-Nasser M, Pandey N, Puig D. Lunginfseg: Segmenting covid-19 infected regions in lung ct images based on a receptive-field-aware deep learning framework. Diagnostics. 2021; 11 (2): 158 . https://doi.org/10.3390/diagnostics11020158

تجزئة الصورة المقطعية للرئة باستخدام شبكة VGG-16 مع تحسين الصورة باستخدام Mittag-Leffler

علي مجيد حسن[1]، محمد ابراهيم خلف [2]، بيان مهدي صبار[3]، رابحة وائل ابراهيم[4,5,6]، حامد عبد الله[6]، فريد مزين[7]

[1]قسم علم وظائف الاعضاء، كلية الطب، جامعة النهرين، بغداد، العراق.
[2]قسم علوم الحاسوب، كلية المعارف الجامعة, الانبار، العراق.
[3]كلية الهندسة والتقنيات الهندسية، جامعة المستقبل، بابل، العراق.
[4]قسم علوم الحاسوب والرياضيات، الجامعة اللبنانية الأميركية، بيروت، لبنان.
[5] قسم الرياضيات، مركز أبحاث الرياضيات، جامعة الشرق الأدنى، مرسين، تركيا.
[6]مجموعة أبحاث تكنولوجيا المعلومات والاتصالات، مركز البحث العلمي، جامعة العين، ذي قار، العراق.
[7]مركز أبحاث علوم البيانات، كلية الحاسبات والهندسة، جامعة ديربي، المملكة المتحدة.

الخلاصة

يعتبر الاستقطاع التلقائي للأمراض خطوة أولية ضرورية في التشخيص الروتيني. تعتبر أمراض الرئة التي تؤثر على الرئتين، مثل الالتهاب الرئوي أو التليف الرئوي والذي يؤدي الى كثافة في أنسجة الرئة والتي تجعل عملية استقطاع هذه المناطق عمليه صعبه جدا بسبب الخصائص المتشابه للانسجة المجاورة. لذا تقترح هذه الدراسة نموذج جديد لاستقطاع الصور المقطعية للرئة والتي تتضمن خطوتين: (1) استخدام نموذج bounded turning Mittag-Leffler لتحسين الصور المقطعية للحصول على نتائج استقطاع أفضل. (2) استخدام شبكة VGG-16 المعدلة لاستقطاع المناطق المصابة بالعدوى في الصور المقطعية للرئة. حيث تم اضافة مجموعة من الطبقات التلافيفية المتوسعة إلى شبكة VGG-16 الأصلية لإنشاء طريقة جديدة لتجزئة صورة الرئة المقطعية. وقد حققت الطريقة المقترحة في هذه الدراسة دقه عالية في عملية الاستقطاع حيث كان معدل الدقه و Dice Coefficient و Jaccard Index هو 96.3%، 91.2%، و82.3% على التوالي. وقد تم مقارنة النتائج المنجزة مع الدراسات السابقة وقد أظهر هذا مدى جودة أداء هذه الدراسة مقارنة بالعديد من الدراسات السابقة على الرغم من ان الحصول على مستوى مناسب من الدقة أمرًا صعبًا للغاية.

الكلمات المفتاحية: تحول محدود، الأشعة المقطعية, تحسين الصورة, وظيفة Mittag-Leffler , شبكة VGG-16.